

# Flows across high aspect ratio street canyons: Reynolds number independence revisited

Lup Wai Chew<sup>1</sup>  · Amir A. Aliabadi<sup>2</sup> · Leslie K. Norford<sup>3</sup>

Received: 14 February 2018 / Accepted: 16 May 2018 / Published online: 22 May 2018  
© Springer Science+Business Media B.V., part of Springer Nature 2018

**Abstract** The Reynolds number for flow in a street canyon,  $Re = U_{ref}H/\nu$  (where  $U_{ref}$  is a reference velocity,  $H$  the street canyon height, and  $\nu$  the kinematic viscosity), cannot be matched between reduced-scale experiments and full-scale field measurements. This mismatch is often circumvented by satisfying the  $Re$  independence criterion, which states that above a critical  $Re$  ( $Re_c$ ), the flow field remains invariant with  $Re$ .  $Re_c = 11,000$  is often adopted in reduced-scale experiments. In deep street canyons with height-to-width aspect ratio  $\geq 1.5$ , reduced-scale experiments have shown two recirculation vortices induced by the mean flows, but full-scale field measurements have observed only one vortex. We investigated this discrepancy by conducting water channel experiments with  $Re$  between  $10^4$  and  $10^5$  at three aspect ratios. The canyons with aspect ratio 1.0 have  $Re_c = 11,000$ , the canyons with aspect ratio 1.5 have  $Re_c$  between 31,000 and 58,000, while the canyons with aspect ratio 2.0 have  $Re_c$  between 57,000 and 87,000. Therefore, the widely adopted  $Re_c = 11,000$  is not applicable for canyons with aspect ratio greater than 1.5. Our results also confirm that there is only one vortex in deep canyons at high  $Re$ . This single-vortex flow regime could change our fundamental understanding of deep canyons, which are often assumed to exhibit multiple-vortex flow regimes. Applications such as numerical model validation based on the multiple-vortex regime should be revisited. Our experimental data with  $Re$  up to  $10^5$  could be used to validate numerical models at high  $Re$ .

**Keywords** Urban street canyons · Water channel experiments · Skimming flow vortex · Critical Reynolds number · Cavity flow · Flow regime transition

---

✉ Lup Wai Chew  
lupwai@mit.edu; chewlupwai@gmail.com

<sup>1</sup> Department of Mechanical Engineering, Massachusetts Institute of Technology, 77 Massachusetts Avenue, 5-418, Cambridge, MA 02139, USA

<sup>2</sup> Environmental Engineering Program, University of Guelph, RICH 2515, Guelph, ON N1G 2W1, Canada

<sup>3</sup> Department of Architecture, Massachusetts Institute of Technology, 77 Massachusetts Avenue, 5-418, Cambridge, MA 02139, USA

## 1 Introduction

Urban street canyons (“canyons” hereafter) are the spaces formed between buildings. They are often simplified in terms of geometry with height  $H$ , width  $W$ , and length  $L$ . When  $L$  is much larger than  $W$ , a two-dimensional (2D) canyon is formed. Due to their poor self-ventilation capability, 2D canyons tend to trap pollutants or heat [5, 27, 35]. For perpendicular wind (i.e., wind blowing in the direction normal to the canyon axis), Oke [31] has categorized flow patterns in 2D canyons in three regimes based on the canyon height-to-width aspect ratio ( $H/W$ ). At  $H/W < 0.3$ , the isolated flow regime is expected, where the effects of the upwind building are isolated from the downwind building. At  $0.3 < H/W < 0.7$ , the wake interference regime is expected, as the wake from the upwind building begins to interfere with the downwind building. At  $H/W > 0.7$ , the skimming flow regime is expected, with one or multiple wind-induced vortices formed in the canyons. Multiple vortices have been observed in deep canyons, i.e., canyons with high aspect ratios ( $H/W \geq 1.5$ ). The skimming flow, also known as cavity flow [16], is the most severe in terms of pollutant or heat trapping inside canyons [5, 22]. Therefore, this paper investigates perpendicular winds across 2D canyons in the skimming flow regime.

Three common approaches to study flow fields in canyons are reduced-scale experiments, in situ field measurements, and numerical modeling. Comprehensive reviews of street canyon modeling are available in Vardoulakis et al. [35] and Ahmad et al. [1]. They highlight that a major limitation of field measurements is the difficulty of decoupling the effects from simultaneously operating parameters in a real built environment. For example, it is difficult to decouple the buoyancy induced by a heated building surface from the measured mean flow [29, 30]. In contrast, reduced-scale experiments allow independent control of each parameter, such as temperature and wind speed. However, reduced-scale experiments cannot meet all the requirements of similitude, including geometric, kinematic, and dynamic similarities of full-scale measurements [2, 16]. The dynamic similarity in momentum requires matching the Reynolds numbers between two experiments. The Reynolds number,  $Re = U_{ref}H/\nu$ , is an important parameter to ensure fully turbulent flow, where  $U_{ref}$  is a reference velocity and  $\nu$  the kinematic viscosity of the fluid. In reduced-scale experiments, scaled-down model blocks with idealized geometry are used to represent buildings in a wind tunnel or water channel. These model blocks often have a geometrical length scale on the order of  $10^{-1}$  m. The corresponding  $Re$  in reduced-scale experiments is on the order of  $10^3$ – $10^4$ . On the other hand, real-size buildings have  $H$  on the order of  $10^1$ – $10^2$  m. With a reference wind speed of  $2 \text{ m s}^{-1}$ , the corresponding  $Re$  is on the order of  $10^5$ – $10^6$ . In order to match this  $Re$  in a wind tunnel with a  $100 \times$  scale reduction, the wind speed required is  $200 \text{ m s}^{-1}$ , which is no longer in the incompressible regime. The mismatch of  $Re$  in reduced-scale experiments is justified by the “Reynolds number independence” hypothesis, stating that as long as the  $Re$  in reduced-scale experiments exceeds a critical value, the normalized flow field remains invariant with increasing  $Re$ . This means that reduced-scale experiments that exceed a critical Reynolds number,  $Re_c$ , could reproduce the flow fields at full scale, since increasing the  $Re$  does not alter the overall normalized flow fields. Assuming this hypothesis is true, the challenging question is to quantify  $Re_c$ .

Next, we outline a few studies that attempted to quantify  $Re_c$ . Castro and Robins [7] conducted wind tunnel tests to study flows across a single cube at different  $Re$ . They found that in a uniform flow,  $Re$  independence is achieved at  $Re_c \sim 30,000$ . In a simulated atmospheric boundary layer flow,  $Re$  independence is achieved at  $Re_c \sim 4000$ . Uehara et al. [34] obtained an  $Re_c \sim 3500$  for  $Re$  independence for a single cube, close to that of

Castro and Robins [7]. Note that the freestream velocity ten cube lengths above the cube was taken as the reference velocity for  $Re_c$  in Castro and Robins [7], while the velocity in an undisturbed flow (i.e., without the cube) at the height of the cube was taken as the reference velocity for  $Re_c$  in Uehara et al. [34]. The  $Re_c$  from both experiments are close to each other, meaning both the above-roof velocity and the velocity in an undisturbed flow are suitable as a reference velocity to calculate  $Re_c$ . Lim et al. [23] conducted wind tunnel experiments and field measurements on a single cube to cover an  $Re$  range spanning two orders of magnitude, from  $2 \times 10^4$  to  $3 \times 10^6$ . They concluded that the normalized mean velocity is independent of  $Re$  within the range of  $Re$  studied. As opposed to a single cube (height-to-width ratio of 1) with an  $Re_c \sim 3500$ , a higher  $Re_c \sim 8000$  was required for a rectangular block with height-to-width ratio of 2 [34], suggesting  $Re$  independence criteria depend on the aspect ratio. Based on a uniform flow across a single cube, Snyder [33] proposed  $Re_c = 11,000$  as a conservative value. Nonetheless, we still lack strong evidence to support the similarity assumption [39]. Although Snyder [33] has warned that experiments with different geometries should derive their own  $Re$  independence criteria,  $Re_c = 11,000$  (or lower, since 11,000 is a “conservative” value) has been widely adopted without questioning its validity for other geometries. In Sect. 2, we will demonstrate the drawback of this assumption after a literature review of reduced-scale experiments and field measurements. The experimental setup is described in Sect. 3. Section 4 discusses the experimental result, followed by conclusions in Sect. 5.

## 2 Literature review

We first review reduced-scale experiments in wind tunnels and water channels (a summary will be provided in Table 1). Gerdes and Olivari [14] visualized the flow fields in canyons with  $H/W$  of 0.7 and 1.0 using Particle Image Velocimetry at an  $Re$  around 4000. They concluded that both values of  $H/W$  produced the same flow pattern, where a single vortex induced by the mean flow was observed. Using Particle Tracking Velocimetry in a water channel, Caton et al. [8] visualized the flow in a canyon with  $H/W$  of 1.0. The  $Re$  was relatively low, between 1000 and 3000. They observed a stable vortex in the canyon, too. Brown et al. [6] conducted a wind tunnel experiment using a 2D array of six canyons with  $H/W$  of 1.0. At an  $Re$  around 30,000, they observed a single vortex in each canyon. Two sets of wind tunnel experiments at  $Re$  between 8000 and 20,000 [28] and between 9500 and 19,000 [20] also revealed one vortex in canyons with  $H/W$  of 1.0. Water channel experiments conducted at an  $Re$  around 10,000 observed one vortex in canyons with  $H/W$  of 1.0 [4, 21], consistent with the wind tunnel experiments. Baik et al. [4] extended their experiments to canyons with  $H/W$  of 1.5, 2.0 and 2.4. In these deep canyons where  $H/W \geq 1.5$ , they observed two vertically aligned, counter-rotating vortices. Experiments by Li et al. [21] on canyons with  $H/W$  of 2.0 at  $Re = 12,000$  also showed two vortices. The top vortex driven by the freestream was stronger than the bottom vortex driven by the top vortex.

Next, we briefly review in situ field measurements in full-scale canyons. There are two major distinctions between reduced-scale experiments and full-scale field measurements. First,  $Re$  in reduced-scale experiments is on the order of  $10^3$ – $10^4$ , whereas  $Re$  in field measurements is on the order of  $10^5$ – $10^6$ . Second, the canyons in reduced-scale experiments are often ideal, whereas real canyons possess three-dimensional features [13, 18, 38] and small-scale structures such as roof shape [15, 36] and roof roughness [3]. Despite the

**Table 1** Summary of reduced-scale experiments (E) and field measurements (F) arranged by canyon height-to-width aspect ratio (H/W)

Authors	E or F*	H (m)	W (m)	H/W	Re	No. of vortices
Gerdes and Olivari [14]	E	0.03	0.045	0.67	4000	1
Caton et al. [8]	E	0.07	0.07	1.0	3000	1
Gerdes and Olivari [14]	E	0.03	0.03	1.0	4000	1
Brown et al. [6]	E	0.15	0.15	1.0	30,000	1
Meroney et al. [28]	E	0.06	0.06	1.0	20,000	1
Kovar-Panskus et al. [20]	E	0.285	0.285	1.0	19,000	1
Baik et al. [4]	E	0.24	0.24	1.0	10,000	1
Li et al. [21]	E	0.1	0.1	1.0	12,000	1
Baik et al. [4]	E	0.24	0.16	1.5	10,000	2
Baik et al. [4]	E	0.24	0.12	2.0	10,000	2
Li et al. [21]	E	0.1	0.05	2.0	12,000	2
Baik et al. [4]	E	0.24	0.10	2.4	10,000	2
Louka et al. [24]	F	4.2	6	0.7	$5.3 \times 10^5$	1
Yamartino and Wiegand [37]	F	18.4	20	0.92	$2.3 \times 10^6$	1
Nakamura and Oke [29]	F	17	16	1.06	$2.1 \times 10^6$	1
Louka et al. [25]	F	21.1 <sup>^</sup>	14.85	1.42	$2.6 \times 10^6$	1
DePaul and Sheih [11]	F	36.75 <sup>^</sup>	24.5	1.5	$4.6 \times 10^6$	1
Eliasson et al. [12]	F	15	7.1	2.1	$1.9 \times 10^6$	1
Santamouris et al. [32]	F	20	8.5	2.35	$2.5 \times 10^6$	1

A reference wind speed of  $2 \text{ m s}^{-1}$  is used to estimate the Re of field measurements

\*E for reduced-scale experiments, F for field measurements

<sup>^</sup>Average of upwind and downwind building heights

non-idealities in real canyons, many field measurements still observed in-canyon vortices under perpendicular winds. Louka et al. [24] reported a single vortex in a canyon with H/W of 0.7. Yamartino and Wiegand [37] reported a single vortex in a canyon with H/W of 0.9 in Cologne, Germany. Nakamura and Oke [29] conducted a field study in a canyon with H/W of about 1.1 in Kyoto, Japan. They reported a single vortex with the highest strength at local standard time 1700 h. These field measurements with H/W near unity or lower are consistent with reduced-scale experiments, which also observed a single vortex. At higher H/W, however, disagreement between them arises. Recall that two vortices were observed in the reduced-scale experiments with H/W of 1.5 and 2.0 [4, 21]. However, in a full-scale canyon with H/W around 1.4, Louka et al. [25] observed only one vortex in the canyon. DePaul and Sheih [11] observed a single vortex in a canyon with H/W around 1.5 by tracking the trajectories of simultaneously released balloons. The core of the vortex was not at the mid-canyon height but shifted upward at about  $0.7H$  above the ground. The single-vortex flow pattern was also observed in field measurements in canyons with  $H/W \geq 2.0$ . In a canyon with H/W around 2.1, Eliasson et al. [12] observed one vortex under quasi-steady perpendicular wind. They also found the core of the vortex at about  $0.7H$  above the ground, similar to DePaul and Sheih [11]. Measuring both wind and temperature in a canyon with H/W about 2.4, Santamouris et al. [32] concluded that a secondary vortex might be induced only when thermal effects (e.g., heated canyon wall) are important. Nonetheless, this does not explain the formation of the secondary vortices in

the reduced-scale experiments, as they were run with isothermal flows with no heated surfaces. Overall, only one vortex is induced in full-scale canyons regardless of the  $H/W$  (in the range of  $H/W$  between 0.7 and 2.4).

This review is summarized in Table 1. For reduced-scale experiments (“E” in the second column), the above-roof-level velocities are well defined, as they are steady and controllable. Correspondingly, the  $Re$  is well defined. In field measurements, however, the above-roof-level winds are often unsteady. We take a wind speed of  $2 \text{ m s}^{-1}$  to calculate the  $Re$ , as some researchers show that a threshold wind speed of  $2 \text{ m s}^{-1}$  is required to sustain the vortex in full-scale canyons [11, 12]. For canyons with  $H/W$  around 1.0 or smaller, the flow patterns seem to be independent of  $Re$ : both reduced-scale experiments ( $Re$  on the order of  $10^3$ – $10^4$ ) and field measurements ( $Re$  on the order of  $10^5$ – $10^6$ ) observed a similar flow pattern with a single vortex. Even at an  $Re$  as low as 3000 [8], the single vortex flow field was still observed. In contrast, for canyons with  $H/W \geq 1.5$ , two vortices were observed in reduced-scale experiments, whereas only one vortex was observed in field measurements. This suggests that flows in canyons with  $H/W \geq 1.5$  have two regimes that are  $Re$  dependent. Referring to Table 1, the transition from the double-vortex regime to the single-vortex regime occurs in the range  $10^4 < Re < 10^6$ . Clearly,  $Re_c = 11,000$  does not apply to canyons with  $H/W \geq 1.5$ , since increasing  $Re$  from  $10^4$  to  $10^6$  changes the flow fields from the double-vortex regime to the single-vortex regime. Unfortunately, if it exists, we are missing the link for the  $Re_c$  between  $10^4$  and  $10^6$ .

The third approach, numerical modeling, covers a wide range of  $Re$  up to  $10^7$ , but numerical models must be validated by experiments or field measurements. Since the inputs to numerical models are controllable, reduced-scale experiments with similar controllable parameters are used for model validation [35]. Such numerical studies therefore make an a priori assumption that the numerical models must reproduce the double-vortex regime in reduced-scale experiments to be considered validated. For example, Baik et al. [4] validated their Computational Fluid Dynamics (CFD) model with their water channel experiments ( $H = 0.24 \text{ m}$ ) and concluded from the CFD simulations that the double-vortex flow exists in a full-scale canyon with  $H = 96 \text{ m}$ . Another example is CFD models that predicted one vortex in full-scale deep canyons were “corrected” to produce the double-vortex regime by employing rough wall functions [19]. Although heated canyon walls could induce a single vortex in a deep canyon [26], under isothermal conditions, the review by Li et al. [22] summarizes that CFD models would predict a single vortex in canyons with  $H/W \leq 1.0$  and two vortices in canyons with  $H/W \geq 1.5$ . Many CFD models have been validated to reproduce the double-vortex flow regime, which may be incorrect should this regime not apply at high  $Re$ . Therefore, we exclude numerical studies from Table 1.

With an increasing number of dense cities expanding vertically, more deep canyons will be created. Therefore, fundamental understanding of flow fields in deep canyons is urgently needed. To understand the fundamentals correctly, we should first establish the criteria for  $Re$  independence in deep canyons, instead of generalizing the criteria from experiments with a single cube. In fact, when providing the  $Re_c = 11,000$  criterion based on flow across a cube, Snyder [33] warned that “tests to establish Reynolds number independence should be an integral part of any model study.” Table 1 shows that reduced-scale experiments of deep canyons were performed at  $Re$  on the order of  $10^4$ , while field measurements had  $Re$  on the order of  $10^6$ . We are missing the link of  $Re$  between  $10^4$  and  $10^6$ , where the transition from two vortices to one vortex occurs. Therefore, we conducted water channel experiments for deep canyons with  $Re$  up to  $10^5$  to fill the gap.

### 3 Experimental setup

All experiments were conducted in a recirculating water channel in the Hydraulic Engineering Laboratory at the Department of Civil and Environmental Engineering, National University of Singapore. Figure 1a shows the side-view sketch of the recirculating water channel, which is 15 m long, 0.6 m tall and 0.6 m wide. A valve controls the flow rate up to a maximum  $50 \text{ L s}^{-1}$ . High flow velocity at the test section was needed to achieve  $Re$  of  $10^5$ , so a partition was installed to reduce the effective width from 0.6 to 0.3 m at the test section. The test section measures 3.6 m long, 0.6 m tall and 0.3 m wide. Flow straighteners made with a combination of plastic tubes, wire mesh and honeycombs were arranged at the inlet to minimize span-wise and vertical velocities. Two layers of ceramic marbles (1.27 cm diameter) accelerated the flow development so the flow profile at the test section was fully developed. The dimensions of the honeycomb and ceramic marbles are shown in Fig. 1b. For the layout of the components upstream (plastic tubes, wire mesh, honeycombs and ceramic marbles), the reader is referred to [9]. The water depth was controlled by the floodgate. The scaled-down model blocks of buildings spanned the full test section width to simulate 2D canyons. Acoustic Doppler Velocimeters (ADV, Vectrino by Nortek AS), were used throughout the experiments to measure all three velocity components (stream-wise, vertical, and span-wise) at the centerlines of canyons 3–6, as shown in Fig. 1c. The ADV were mounted on metal frames with adjustable vertical position. The diameter of the probe is 8 mm. The sampling volume diameter is 6 mm. The accuracy is  $\pm 1 \text{ mm s}^{-1} \pm 0.5\%$  of measured value (e.g., if the measured value is  $200 \text{ mm s}^{-1}$ , the accuracy is  $\pm 1 \text{ mm s}^{-1} \pm 0.5\% \times 200 \text{ mm s}^{-1} = \pm 2 \text{ mm s}^{-1}$ ).

The scaled-down model blocks of buildings were made of marine plywood coated with epoxy. Three sets of experiments were conducted at  $H/W$  of 1.0, 1.5 and 2.0. The dimensions

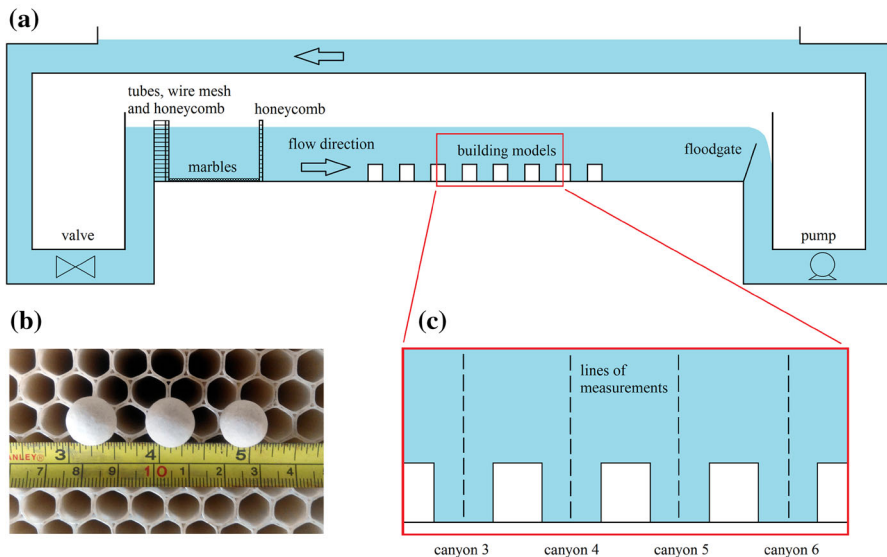


**Fig. 1** a Side view of the recirculating water channel with an adjustable floodgate and a control valve to vary the flow rate and water level. The models of buildings were placed in the middle of the test section. b Dimensions of the honeycomb and ceramic marbles (top scale in inches, bottom scale in centimeters). c Centerlines of canyons 3–6, where the velocity profiles were measured

of model blocks and canyons are summarized in Table 2. For canyons with H/W of 1.0, seven canyons of 0.12 m by 0.12 m were formed between eight model blocks of 0.12 m by 0.10 m. For canyons with H/W of 1.5, six canyons of 0.20 m by 0.13 m were formed between seven model blocks of 0.20 m by 0.12 m. For canyons with H/W of 2.0, six canyons of 0.20 m by 0.10 m were formed between seven model blocks of 0.20 m by 0.12 m. The measurement frequency was at least 50 Hz and the measurement period was at least 60 s, which have been verified to be sufficient to obtain both the mean velocities and turbulence based on the advection time scale [10]. The advection time scale can be estimated as  $H/U_{ref}$ . A small advection time scale requires higher measurement frequency, while a large advection time scale requires longer averaging period. The measurement frequency was increased to 100 Hz for the case with the smallest advection time scale, while the measurement period was increased to 360 s for the case with the largest advection time scale.

Due to the limitation of the ADV probes, the spacing between two model blocks must exceed 0.06 m (i.e.,  $W > 0.06$  m). We modeled canyons with H/W of 1.0 with  $H = W = 0.12$  m. For canyons with H/W of 2.0, we could not reduce  $W$  to 0.06 m (while maintaining  $H = 0.12$  m) due to the probe limitation. Therefore, we modeled them with  $H = 0.20$  m and  $W = 0.10$  m. The water channel has a maximum water depth of 0.55 m. In terms of  $H$ , the maximum water depths for experiments with H/W of 1.0 (where  $H = 0.12$  m) and H/W of 1.5 and 2.0 (where  $H = 0.20$  m) are  $4.58H$  and  $2.75H$ , respectively. The water channel experiments in Li et al. [21] and Baik et al. [4] had water depths of  $4H$  and  $1.4H$ . Therefore, the water depth of  $2.75H$  in our experiments is lower than that in Li et al. [21] but double that in Baik et al. [4]. The Froude number ( $Fr$ ) based on the water depth and reference velocity was between 0.025 and 0.26. We conducted a sensitivity study on the effects of water depth, which will be discussed in Sect. 4.1.

### 4 Results and discussion

This section discusses the experimental results. All three components of velocity were measured. The mean velocities were calculated by time averaging the velocities over the whole measurement periods. The mean stream-wise velocity,  $u$ , and the mean vertical velocity,  $w$ , are reported. The mean span-wise velocity,  $v$ , was zero due to span-wise symmetry and is not plotted. We also report the Reynolds stress,  $u'w'$ , and the turbulence kinetic energy,  $TKE = 0.5(u'^2 + v'^2 + w'^2)$ , where  $u'$ ,  $v'$ , and  $w'$  are the root-mean-squared stream-wise, span-wise, and vertical velocity fluctuations, respectively. The mean velocities are normalized by a reference velocity,  $U_{ref}$ , which is the freestream velocity at

**Table 2** Dimensions of model blocks and canyons in the experiments at three aspect ratios, H/W

H/W	H (m)	W (m)	Block W (m)	Water depth (m)	No. of canyons	Re range	Fr range
1.0	0.12	0.12	0.10	0.24, 0.40	7	19,000–62,000	0.083–0.26
1.5	0.20	0.13	0.12	0.55	6	12,000–106,000	0.027–0.22
2.0	0.20	0.10	0.12	0.55	6	12,000–105,000	0.025–0.22

$H$  is the height of canyons (similar to the height of model blocks),  $W$  is the width of canyons, Block  $W$  is the width of model blocks,  $Re$  is the Reynolds number, and  $Fr$  is the Froude number

least  $2H$  above the canyon ground, as recommended by Kastner-Klein et al. [17] and Li et al. [21]. The Reynolds stress and TKE are normalized by  $U_{ref}^2$ .

#### 4.1 Canyon with aspect ratio of 1.0

Figure 2 summarizes the experimental results for canyons with  $H/W$  of 1.0. The water channel experiment in Li et al. [21] with  $H = W = 0.1$  m and  $Re = 12,000$  is included for comparison. The experiment in Li et al. [21] used Laser Doppler Velocimetry (LDV), which is non-intrusive; while our experiments used ADV, which is categorized as an intrusive measuring device. The agreement between their LDV and our ADV measurements verified that the presence of the ADV probes in our experiments did not affect the results. The runs with  $Re = 19,000$  and  $Re = 62,000$  had a water depth of  $0.4$  m =  $3.3H$ , with corresponding  $Fr = 0.083$  and  $Fr = 0.26$ . A sensitivity study on the effects of water

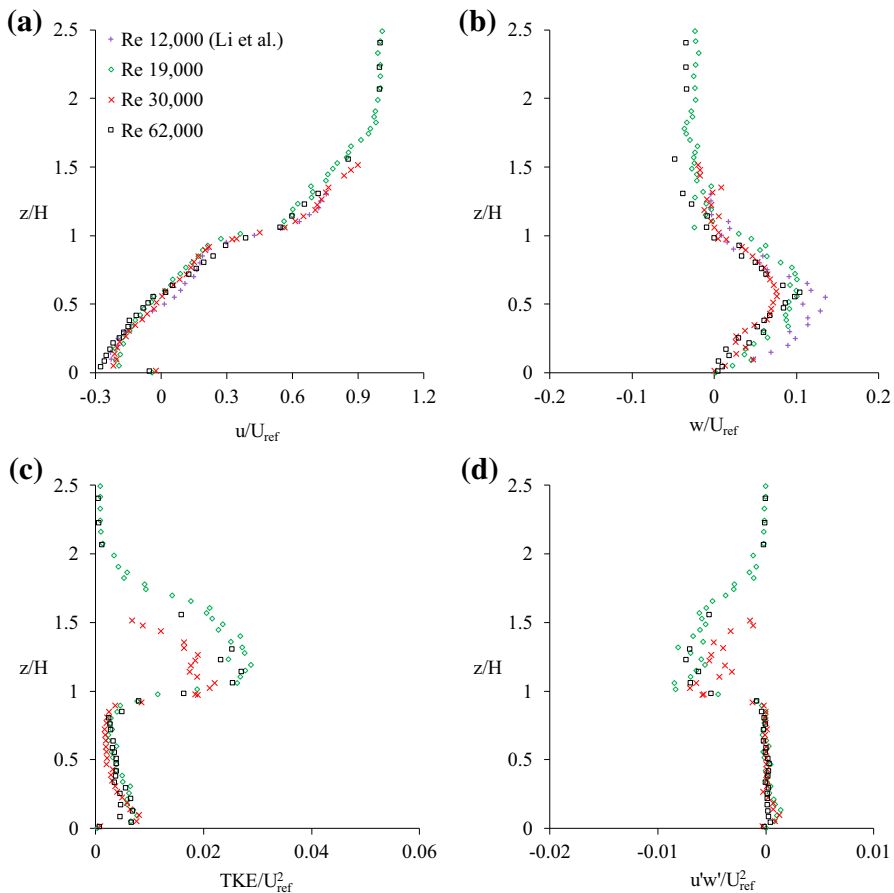


**Fig. 2** Normalized profiles for canyons with aspect ratio of 1.0. **a** Mean stream-wise velocity, **b** mean vertical velocity, **c** turbulence kinetic energy, and **d** Reynolds stress. Water channel data from Li et al. [21] are included in **a** and **b**. All profiles were measured at the centerline of the fourth canyon. The  $Re$  12,000 case has a water depth of  $4.0H$ , the  $Re$  19,000 and 62,000 cases have a water depth of  $3.3H$ , the  $Re$  30,000 case has a water depth of  $2.0H$

depth was conducted with a water depth of  $0.24 \text{ m} = 2.0H$  with a corresponding  $Fr = 0.15$  for the run with  $Re = 30,000$ . The case with  $Re = 12,000$  in Li et al. [21] had a water depth of  $4.0H$ . To ensure repeatability of the experimental setup, the case with  $Re = 19,000$  was repeated two times on two separate days. All three runs produced identical results, with negligibly small run-to-run standard deviations (0.6% of  $U_{ref}$  for mean velocities and 0.3% of  $U_{ref}$  for velocity fluctuations), confirming the repeatability of the experimental setup. Brown et al. [6] and Meroney et al. [28] showed that in a series of canyons, the first two canyons exhibit different flow fields compared to the third and downstream canyons. We measured the velocity profiles in the third to sixth canyons, and verified that they are similar. For brevity, only the profiles in the fourth canyon are shown.

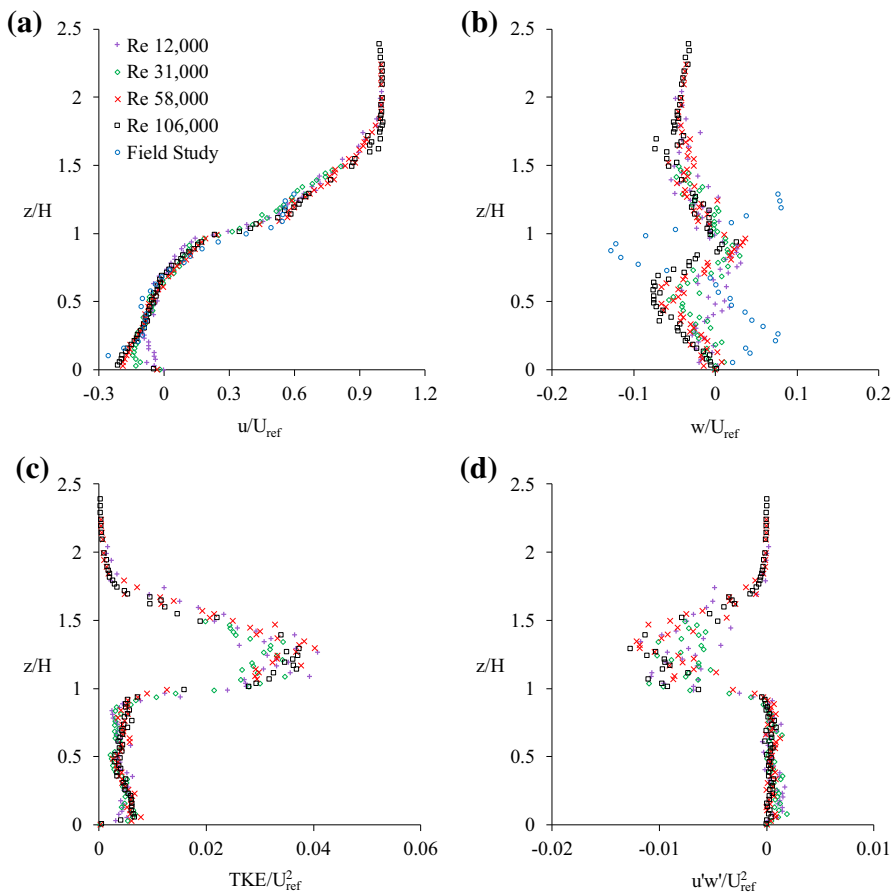
Figure 2a shows that  $u/U_{ref}$  is  $Re$  independent in the range of  $Re$  between 12,000 and 62,000. The freestream flow in the positive  $x$ -direction (i.e., positive  $U_{ref}$ ) drives a clockwise rotating vortex, which induces negative  $u/U_{ref}$  near the bottom. Reducing the water depth from  $3.3H$  (the cases with  $Re = 19,000$  and  $Re = 62,000$ ) to  $2H$  (the case with  $Re = 30,000$ ) does not affect  $u/U_{ref}$  profiles. Increasing the  $Fr$  from 0.083 to 0.26 does not affect  $u/U_{ref}$  profiles, confirming the free surface effect is negligible even at the largest  $Fr = 0.26$ . Figure 2b shows  $w/U_{ref}$  is positive inside the canyon ( $z/H < 1$ ). This suggests that the vortex is asymmetric, with its core slightly offset from the center of the canyon. Both  $u/U_{ref}$  and  $w/U_{ref}$  are zero at the bottom, satisfying the no-slip condition. The mean span-wise velocity is zero (not shown).

Figure 2c shows that the normalized TKE remains almost constant inside the canyon ( $z/H < 1$ ) except near the bottom, where TKE is slightly higher. At the bottom, TKE decays to zero, as expected. The TKE peaks at the roof level ( $z/H = 1$ ) and decays with increasing  $z/H$ . The water depth has no significant effect on TKE inside the canyon, but the  $Re = 30,000$  case with  $2H$  water depth had lower normalized TKE above the roof level. The ADV probe could measure only 5 cm or deeper below the water surface, so no data was acquired near the water surface (above  $z/H = 1.6$ ) for this case. Figure 2d shows that the normalized Reynolds stress,  $u'w'/U_{ref}^2$ , remains zero inside the canyon and above  $z/H = 2$ , but peaks at the roof level. The case with  $2H$  water depth ( $Re = 30,000$ ) shows a faster decay of Reynolds stress with increasing  $z/H$ , possibly due to the smaller water depth. Note that the case with  $Re = 30,000$  and  $2H$  water depth (which shows a faster decay of TKE and Reynolds stress above the roof level) had  $Fr = 0.15$ . The case with  $Re = 62,000$  had a larger  $Fr = 0.26$ , but does not show such decay. This suggests that the water depth (relative to the canyon height) plays a more important role on this decay when  $Fr$  is smaller than 0.26.

In this study, we consider  $Re$  independence is achieved when the mean velocity profiles do not change with increasing  $Re$ . Overall, all profiles in Fig. 2a–d show no apparent change in the flow pattern from  $Re = 12,000$  to  $Re = 62,000$ , confirming that flows in canyons with  $H/W$  of 1.0 achieve  $Re$  independence at  $Re > 11,000$ . This criterion for  $Re$  independence is widely adopted in the literature [4, 21, 28, 33]. On the effects of water depth, reducing the water depth from  $3.3H$  to  $2H$  did not change the mean velocity profiles, but the normalized TKE and Reynolds stress are slightly reduced above the roof level. Since this study investigates  $Re$  independence based on the mean velocities and the number of vortices inside a canyon, lower normalized TKE and Reynolds stress above the roof level are not a concern. However, for studies where above-roof turbulence is important, a water depth larger than  $2H$  and  $Fr$  smaller than 0.15 are recommended.

## 4.2 Canyon with aspect ratio of 1.5

Figure 3 summarizes the experimental results for canyons with  $H/W$  of 1.5. All runs had a water depth of  $2.75H$  and  $Fr \leq 0.22$ . The field measurement from DePaul and Sheih [11] is included in the mean profiles (a) and (b) for comparison. Note that DePaul and Sheih [11] adopted the wind speed at  $1.3H$  as their reference velocity. To directly compare their data with ours (we used the freestream velocity above  $2H$  as  $U_{ref}$ ), we scaled the normalized velocity in DePaul and Sheih [11] by a factor of 0.6, since the velocity at  $1.3H$  is about 60% of the velocity at  $2H$ . Figure 3a shows that above  $z/H = 0.3$ , the profiles of  $u/U_{ref}$  do not change significantly with increasing  $Re$ . On the other hand, below  $z/H = 0.3$ ,  $u/U_{ref}$  is the lowest at the smallest  $Re = 12,000$ . When  $Re$  is increased to 31,000, the magnitude of  $u/U_{ref}$  increases. A further increase of  $Re$  to 58,000 results in a further increase of  $u/U_{ref}$  in magnitude. At the highest  $Re = 106,000$ , the profile is similar to that of  $Re = 58,000$ . This suggests that the  $Re_c$  for the flow to be  $Re$  independent is between 31,000 and 58,000 for



**Fig. 3** Normalized profiles for canyons with aspect ratio of 1.5. **a** Mean stream-wise velocity, **b** mean vertical velocity, **c** turbulence kinetic energy, and **d** Reynolds stress. The field study in **a** and **b** had an  $Re$  about  $1.4 \times 10^7$  [11]. All profiles (except the field study) were measured at the centerline of the fourth canyon

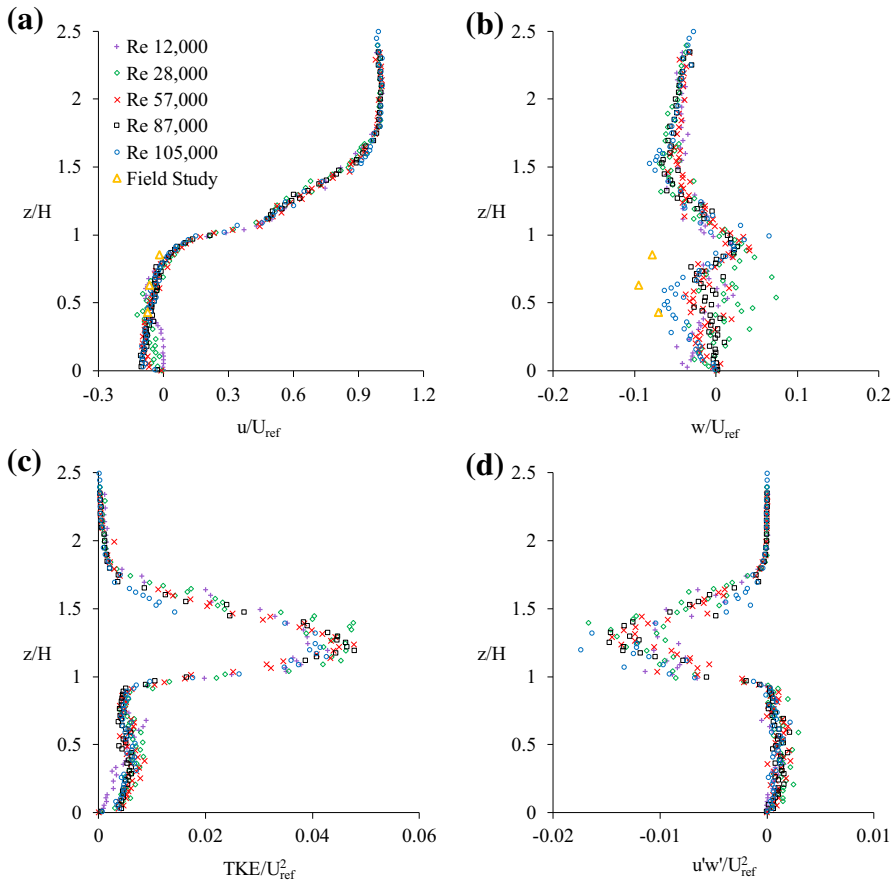
canyons with  $H/W$  of 1.5. Our  $u/U_{\text{ref}}$  profiles for the two largest  $Re$  show good agreement with the field measurement, which has an  $Re$  around  $1.4 \times 10^7$ . In addition, all  $u/U_{\text{ref}}$  profiles show negative  $u/U_{\text{ref}}$  near the bottom, indicating that there is only one vortex in the canyon. If there were a second vortex, the velocity near the bottom would be positive, as the bottom vortex would rotate counterclockwise. Figure 3b shows that in general,  $w/U_{\text{ref}}$  is very small and does not depend on  $Re$ . The larger mismatch between our experimental profiles with the field measurement is due to the asymmetric canyon in the latter. The canyon studied by DePaul and Sheih [11] is a “step-up” canyon [35] with a shorter upwind wall (33.5 m) and a taller downwind wall (40 m). The vertical velocity is more sensitive to the asymmetry of a canyon than the stream-wise velocity [10]. Figure 3c, d show that the normalized TKE and Reynolds stress profiles do not depend on  $Re$ , with their peaks recorded near the roof level. Overall, the canyon with  $H/W$  of 1.5 at  $Re \geq 58,000$  shows very similar flow profiles to that of a canyon with  $H/W$  of 1.0. Since further increasing the  $Re$  to 106,000 did not result in a significant change in the  $u/U_{\text{ref}}$  profile, our experiments suggest that  $Re_c$  is between 31,000 and 58,000 for canyons with  $H/W$  of 1.5.

Next, we will demonstrate that a higher canyon height-to-length ratio ( $H/L$ ) in our experiments does not affect the outcome. Recall that canyons with  $H/W$  of 1.0 have  $H = 0.12$  m, while canyons with  $H/W$  of 1.5 have  $H = 0.20$  m (see Table 2). The canyon length,  $L$ , is 0.3 m, so increasing  $H$  from 0.12 to 0.20 m increases  $H/L$  from 0.40 to 0.67. To ensure that this increase in  $H/L$  does not affect the results, we repeated the experiments with  $Re$  at 12,000, 31,000 and 58,000 with canyons of  $H = 0.12$  m and  $W = 0.08$  m (i.e.,  $H/L$  of 0.40, with  $H/W$  maintained at 1.5). All three sets of experiments produced similar results at  $H/L$  of 0.40 and 0.67, verifying that the increase in  $H/L$  has negligible effects on the experiments.

### 4.3 Canyon with aspect ratio of 2.0

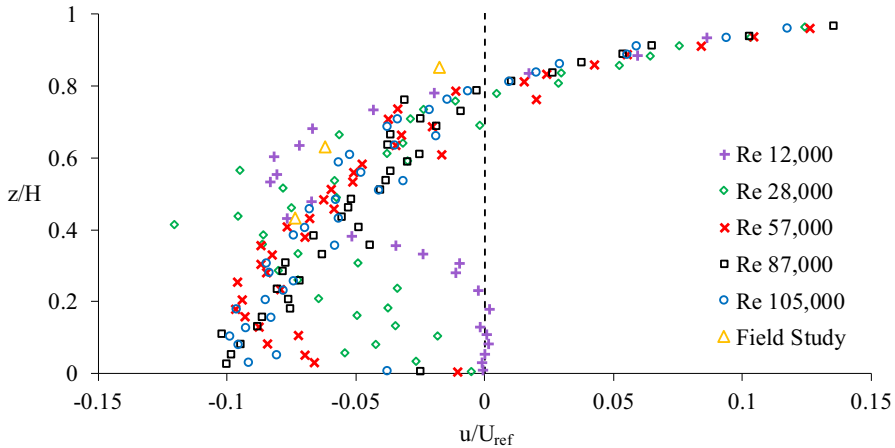
Figure 4 summarizes the experimental results for canyons with  $H/W$  of 2.0. All runs had a water depth of  $2.75H$  and  $Fr \leq 0.22$ . The field measurement of a full-scale canyon with  $H/W$  of 2.1 in Eliasson et al. [12] is included for the mean velocity profiles (only the start hour 16 of Fig. 4 in Eliasson et al. [12] was selected, as it represents a perpendicular wind with negligible along-canyon wind). Figure 4a shows that  $u/U_{\text{ref}}$  is independent of  $Re$  above  $z/H = 0.4$ . Below  $z/H = 0.4$ , the case with the lowest  $Re = 12,000$  has almost zero velocity while the high  $Re$  cases ( $\geq 57,000$ ) show  $u/U_{\text{ref}}$  of about  $-0.1$ . As  $u/U_{\text{ref}}$  is the most important parameter to determine the number of vortices in the canyon, we will discuss  $u/U_{\text{ref}}$  in detailed in the next paragraph. Figure 4b shows that there is no apparent change in  $w/U_{\text{ref}}$  with increasing  $Re$ . Our experiments show smaller magnitudes of  $w/U_{\text{ref}}$  compared to the field measurement but the difference is small. Figure 4c shows that the normalized TKE is the highest between  $z/H = 1$  and  $z/H = 2$ . Above  $z/H = 2$ , TKE decays rapidly. Above  $z/H = 0.4$ , the normalized TKE is independent of  $Re$ . Below  $z/H = 0.4$ , the lowest  $Re$  case has the smallest normalized TKE. Increasing  $Re$  to 28,000 increases the normalized TKE below  $z/H = 0.4$ . Further increasing the  $Re$  to 57,000 and higher did not change the overall profiles, suggesting that only the case with the lowest  $Re = 12,000$  has a different flow structure in the canyon. Figure 4d shows that the normalized Reynolds stress is near zero inside the canyon ( $z/H < 1$ ) and increases rapidly at the roof level, with peaks between  $z/H = 1$  and  $z/H = 1.5$ . There is no apparent change of normalized Reynolds stress with increasing  $Re$ .

Figure 5 replots  $u/U_{\text{ref}}$  in Fig. 4a by zooming into the in-canyon region ( $z/H < 1$ ) and using a smaller x-axis range to emphasize the trend with increasing  $Re$ . The field



**Fig. 4** Normalized profiles for canyons with aspect ratio of 2.0. **a** Mean stream-wise velocity, **b** mean vertical velocity, **c** turbulence kinetic energy, and **d** Reynolds stress. The field study in **a** and **b** had an Re about  $2.7 \times 10^6$  [12]. All profiles (except the field study) were measured at the centerline of the fourth canyon

measurement in a real canyon of  $H/W$  of 2.1 has an Re about  $2.7 \times 10^6$  [12]. From Table 1, there is only one vortex in the real canyon with Re on the order of  $10^6$ , whereas there are two vortices in the reduced-scale canyons with Re on the order of  $10^4$ . Our experiments cover a range of Re between  $10^4$  and  $10^5$ . Two interesting features can be observed in Fig. 5. First, at the lowest Re = 12,000, the peak negative  $u/U_{ref}$  is near  $z/H = 0.6$ . The magnitude of  $u/U_{ref}$  decreases with decreasing  $z/H$  and approaches zero near  $z/H = 0.3$ . Between  $z/H = 0.1$  and  $z/H = 0.2$ , there is very small positive  $u/U_{ref}$  recorded. If there is a single vortex in a canyon (with positive freestream velocity), the near-ground velocity would be negative, similar to the cases with  $H/W$  of 1.0 discussed in Sect. 4.1 (see Fig. 2a). The  $u/U_{ref}$  profile at the lowest Re = 12,000 suggests that two vortices are induced, but the bottom vortex is significantly weaker. The top vortex occupies the top part of the canyon between  $z/H = 0.4$  and  $z/H = 1$ , while the bottom vortex occupies the bottom part of the canyon below  $z/H = 0.4$ . The core of the top vortex (where



**Fig. 5** Normalized mean stream-wise velocity for canyons with aspect ratio of 2.0. The field study is from Eliasson et al. [12] and has an  $Re$  about  $2.7 \times 10^6$ . At the lowest  $Re = 12,000$ , flow below  $z/H = 0.3$  is very weak and could be positive, indicating a bottom vortex.  $Re$  independence is achieved between  $Re = 57,000$  and  $Re = 87,000$ , since increasing  $Re$  from 87,000 to 105,000 does not result in a change in  $u/U_{ref}$  profiles

$u/U_{ref}$  approaches zero) is located near  $z/H = 0.75$ , close to the location in the reduced-scale experiments ( $z/H = 0.78$ ) in Baik et al. [4].

The second feature is the sign of near-ground  $u/U_{ref}$ , which helps to determine the number of vortices in a canyon. Negative near-ground  $u/U_{ref}$  indicates that there is only one vortex in the canyon. The transition to the single vortex flow regime is observed at  $Re = 28,000$ . The profile at  $Re = 28,000$  shows a higher scatter, suggesting the transition could be unstable with intermittent switching between single vortex and double vortex. The profiles with  $Re = 57,000$ ,  $Re = 87,000$ , and  $Re = 105,000$  show negative near-ground  $u/U_{ref}$ , indicating that only one vortex was induced in the canyon in each case. The cores of these single vortices are located near  $z/H = 0.75$ , within the range of the field measurement (between  $z/H = 0.63$  and  $z/H = 0.85$ ) [12]. The case with  $Re = 28,000$  has its peak negative  $u/U_{ref}$  near  $z/H = 0.4$ . The case with a higher  $Re = 57,000$  has its peak negative  $u/U_{ref}$  shifted downward near  $z/H = 0.2$ . Further increasing  $Re$  to 87,000 shifts the peak negative  $u/U_{ref}$  to near the ground level. The case with the highest  $Re = 105,000$  also has its peak negative  $u/U_{ref}$  near the ground. Overall, the lowest  $Re$  case shows  $u/U_{ref}$  profile with a top vortex and a very weak bottom vortex, while all other cases show  $u/U_{ref}$  profiles with a single vortex. Below  $z/H = 0.4$ , increasing  $Re$  from 12,000 to 87,000 changes  $u/U_{ref}$  profiles in terms of the locations of their peak magnitude. Since further increasing  $Re$  to 105,000 did not result in a significant change in the  $u/U_{ref}$  profile, our experiments suggest that  $Re_c$  is between 57,000 and 87,000 for canyons with  $H/W$  of 2.0.

#### 4.4 Comparison of canyons with different aspect ratios

The previous subsections discuss the results of canyons with  $H/W$  of 1.0, 1.5 and 2.0 separately. At high  $Re$ , there is only one vortex in canyons with  $H/W$  of 1.5 and 2.0, similar to canyons with  $H/W$  of 1.0. This means the flow fields in deep canyons could be similar to that of the well-studied canyons with  $H/W$  of 1.0, provided the  $Re$  exceeds a critical value. To make a direct comparison at different  $H/W$ , Fig. 6 plots the normalized profiles at the lowest and highest  $Re$  in canyons with  $H/W$  of 1.0, 1.5 and 2.0. The first points nearest to

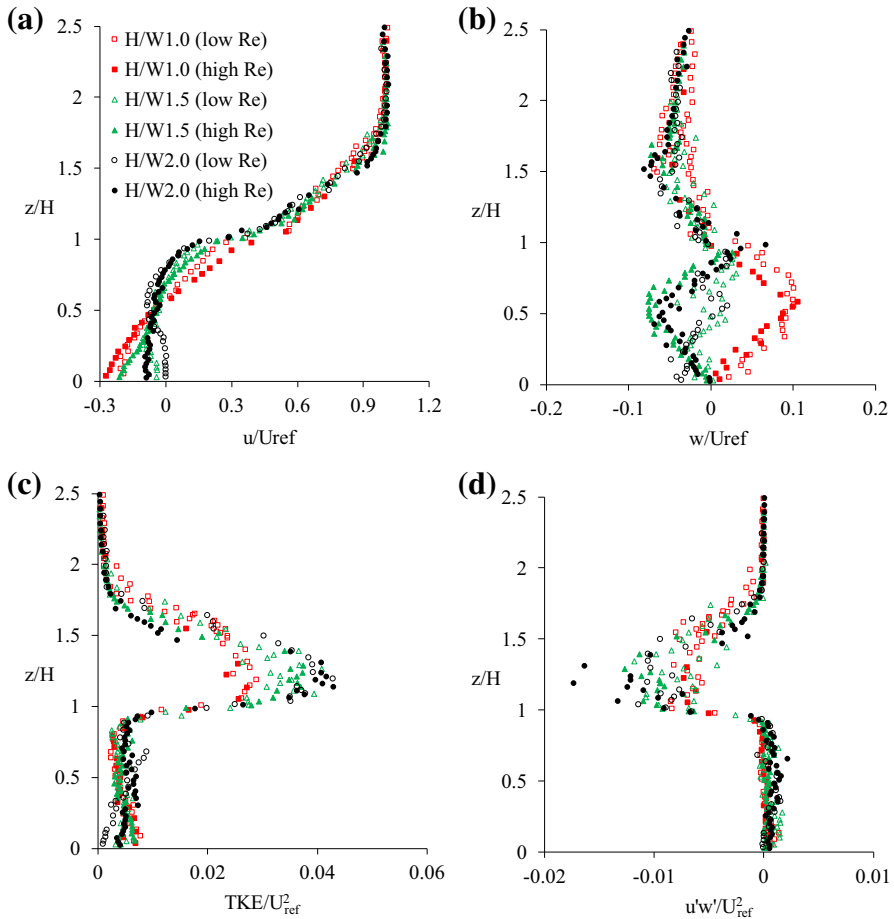


**Fig. 6** Normalized profiles at aspect ratios ( $H/W$ ) of 1.0, 1.5 and 2.0, comparing cases with the lowest and highest Reynolds numbers at each aspect ratio. **a** Mean stream-wise velocity, **b** mean vertical velocity, **c** turbulence kinetic energy, and **d** Reynolds stress

the ground were removed to ease comparisons, as all cases have these points very close to zero (satisfying the no-slip condition at the ground). For  $H/W$  of 1.0, the low Re and high Re cases have  $Re = 19,000$  and  $Re = 62,000$ . For  $H/W$  of 1.5, the low Re and high Re cases have  $Re = 12,000$  and  $Re = 106,000$ . For  $H/W$  of 2.0, the low Re and high Re cases have  $Re = 12,000$  and  $Re = 105,000$ . Open symbols represent low Re cases, while filled symbols represent high Re cases.

Figure 6a shows that for canyons with  $H/W$  of 1.0, the overall profiles remain unchanged from low Re to high Re, although the near-ground  $u/U_{ref}$  magnitude is slightly higher in the high Re case. There is only one vortex in the canyon, and the peaks of  $u/U_{ref}$  (in magnitude) are near the ground at both low Re and high Re. In contrast, for canyons with  $H/W$  of 2.0, the low Re case has a different profile than the high Re case. At low Re, the top vortex occupies the canyon space between  $z/H = 0.4$  and  $z/H = 1.0$ . Below  $z/H = 0.4$ ,  $u/U_{ref}$  is near zero, so there is either no flow or a very weak bottom vortex in this region. On the other hand, at high Re, the  $u/U_{ref}$  profile shows negative near-ground  $u/U_{ref}$ ,

**Table 3** The critical Reynolds number ( $Re_c$ ), the highest Reynolds number ( $Re$ ) in our experiments, the number of vortices observed at the highest  $Re$ , and the location of the cores of these vortices at aspect ratios ( $H/W$ ) 1.0, 1.5, and 2.0

$H/W$	$Re_c$	Highest $Re$ in experiments	No. of vortices at highest $Re$	Location of vortex core ( $z/H$ )
1.0	11,000	62,000	1	0.55
1.5	Between 31,000 and 58,000	106,000	1	0.70
2.0	Between 57,000 and 87,000	105,000	1	0.75

with its peak (in magnitude) near the ground. A similar trend is observed for the canyons with  $H/W$  of 1.5. Comparing  $u/U_{ref}$  profiles at high  $Re$ , although all  $H/W$  cases exhibit profiles resembling a single vortex, there is a major difference: the location of the core of the vortex. For canyons with  $H/W$  of 1.0, the vortex core is near the mid-canyon height at  $z/H = 0.55$ , whereas for canyons with  $H/W$  of 1.5 and 2.0, the cores are located near  $z/H = 0.70$  and  $z/H = 0.75$ . Figure 6b shows that  $w/U_{ref}$  depends on  $H/W$  but not  $Re$ . Figure 6c shows that the normalized TKE profiles are almost the same, except the case with  $H/W$  of 2.0 at low  $Re$ . Below  $z/H = 0.4$ , the normalized TKE is lower at low  $Re$ . This is again due to a very weak flow in the lower region at low  $Re$ . Lastly, the normalized Reynolds stress profiles in Fig. 6d do not show any relationship with  $H/W$  or  $Re$ . All profiles show negligible Reynolds stress inside the canyon ( $z/H < 1$ ) and peak between  $z/H = 1$  and  $z/H = 1.5$ .

### 5 Conclusions

We revisited the critical Reynolds number ( $Re_c$ ) required to satisfy Reynolds number ( $Re$ ) independence with 2D idealized canyons at aspect ratios ( $H/W$ ) of 1.0, 1.5 and 2.0. From the literature, only one vortex is induced by the mean flow in canyons with  $H/W$  near unity or lower for both reduced-scale experiments ( $Re$  on the order of  $10^3$ – $10^4$ ) and field measurements ( $Re$  on the order of  $10^5$ – $10^6$ ). In contrast, for deep canyons with  $H/W \geq 1.5$ , reduced-scale experiments ( $Re$  on the order of  $10^4$ ) observe two vortices while field measurements ( $Re$  on the order of  $10^6$ ) report only one vortex. There were no data available for deep canyons with  $Re$  on the order of  $10^5$ . We conducted water channel experiments up to  $Re \sim 10^5$  to fill this gap. The key observations are summarized in Table 3. For canyons with  $H/W$  of 1.0, the in-canyon flows are independent of  $Re$  at  $Re$  above 12,000, confirming the widely adopted  $Re$  independence criterion ( $Re_c = 11,000$ ). For canyons with  $H/W$  of 1.5,  $Re$  independence is achieved between  $Re = 31,000$  and  $Re = 58,000$  in our experiments. For canyons with  $H/W$  of 2.0,  $Re$  independence is achieved between  $Re = 57,000$  and  $Re = 87,000$ . At the highest  $Re$ , only one vortex was observed in each case, regardless of the  $H/W$ . A direct comparison of the mean stream-wise velocity profiles among all cases shows that the flow structures in deep canyons at  $Re$  above  $10^5$  are similar to that of canyons with  $H/W$  of 1.0, but the cores of the vortices in deep canyons are shifted upward.

From the above observations, we made two conclusions. First,  $Re_c = 11,000$  for  $Re$  independence is satisfied only for canyons with  $H/W \leq 1.0$ . For canyons with  $H/W$  of 1.5, our experiments show that  $Re = 58,000$  is sufficient for  $Re$  independence. For canyons with  $H/W$  of 2.0,  $Re = 87,000$  is sufficient for  $Re$  independence. This suggests that the  $Re_c$

required for Re independence is a function of  $H/W$ . A more appropriate length scale should include both  $H$  and  $W$  in the definition of Re. For example, the hydraulic diameter  $HW/(W + 2H) = H/(1 + 2H/W)$  could be a suitable length scale. The second conclusion from our experiments is that at high Re, there is only one vortex in deep canyons, consistent with full-scale field measurements. This is contrary to reduced-scale experiments that reported two vortices (at low Re). Since full-scale deep canyons exhibit a single-vortex flow pattern, we should revisit studies of deep canyons that were based on the double-vortex flow regime. CFD models are often validated with low Re experiments that exhibit the double-vortex flow regime, and thus some “validated” CFD models predict two vortices in deep canyons. We provide experimental data for deep canyons at a range of Re up to  $10^5$  and encourage the revalidation of CFD models to correctly predict a single vortex in deep canyons at high Re.

**Acknowledgements** This research is supported by the National Research Foundation Singapore under its Campus for Research Excellence and Technological Enterprise programme. The authors thank Prof. Rajasekhar Balasubramanian and Dr. Kian Yew Lim for discussions on the experimental setup and result analyses. Help from the technical staff in the Hydraulic Engineering Laboratory is acknowledged.

## References

1. Ahmad K, Khare M, Chaudhry K (2005) Wind tunnel simulation studies on dispersion at urban street canyons and intersections—a review. *J Wind Eng Ind Aerodyn* 93:697–717
2. Aliabadi AA (2018) Theory and applications of turbulence: a fundamental approach for scientists and engineers. Amir A. Aliabadi Publications, Guelph
3. Aliabadi AA, Krayenhoff ES, Nazarian N, Chew LW, Armstrong PR, Afshari A, Norford LK (2017) Effects of roof-edge roughness on air temperature and pollutant concentration in urban canyons. *Bound Layer Meteorol* 164:1–31
4. Baik J-J, Park R-S, Chun H-Y, Kim J-J (2000) A laboratory model of urban street-canyon flows. *J Appl Meteorol* 39:1592–1600
5. Britter R, Hanna S (2003) Flow and dispersion in urban areas. *Annu Rev Fluid Mech* 35:469–496
6. Brown MJ, Lawson RE, DeCroix DS, Lee RL (2000) Mean flow and turbulence measurements around a 2-D array of buildings in a wind tunnel. In: 11th Joint AMS/AWMA conference on the applications of air pollution meteorology. Long Beach, CA
7. Castro I, Robins A (1977) The flow around a surface-mounted cube in uniform and turbulent streams. *J Fluid Mech* 79:307–335
8. Caton F, Britter RE, Dalziel S (2003) Dispersion mechanisms in a street canyon. *Atmos Environ* 37:693–702
9. Chew LW (2017) Passive enhancement of air flow at pedestrian level in built environments. Master thesis, Massachusetts Institute of Technology
10. Chew LW, Nazarian N, Norford L (2017) Pedestrian-level urban wind flow enhancement with wind catchers. *Atmosphere* 8:159
11. DePaul F, Sheih C (1986) Measurements of wind velocities in a street canyon. *Atmos Environ* 1967 20:455–459
12. Eliasson I, Offerle B, Grimmond C, Lindqvist S (2006) Wind fields and turbulence statistics in an urban street canyon. *Atmos Environ* 40:1–16
13. Fernando H, Lee S, Anderson J, Princevac M, Pardyjak E, Grossman-Clarke S (2001) Urban fluid mechanics: air circulation and contaminant dispersion in cities. *Environ Fluid Mech* 1:107–164. <https://doi.org/10.1023/A:1011504001479>
14. Gerdes F, Olivari D (1999) Analysis of pollutant dispersion in an urban street canyon. *J Wind Eng Ind Aerodyn* 82:105–124
15. Huang Y, Hu X, Zeng N (2009) Impact of wedge-shaped roofs on airflow and pollutant dispersion inside urban street canyons. *Build Environ* 44:2335–2347
16. Kanda M (2006) Progress in the scale modeling of urban climate. *Theor Appl Climatol* 84:23–33
17. Kastner-Klein P, Fedorovich E, Rotach M (2001) A wind tunnel study of organised and turbulent air motions in urban street canyons. *J Wind Eng Ind Aerodyn* 89:849–861

18. Klein P, Clark JV (2007) Flow variability in a North American downtown street canyon. *J Appl Meteorol Climatol* 46:851–877
19. Koutsourakis N, Bartzis JG, Markatos NC (2012) Evaluation of Reynolds stress,  $k-\epsilon$  and RNG  $k-\epsilon$  turbulence models in street canyon flows using various experimental datasets. *Environ Fluid Mech* 12:379–403. <https://doi.org/10.1007/s10652-012-9240-9>
20. Kovar-Panskus A, Moulinneuf L, Savory E, Abdelqari A, Sini J-F, Rosant J-M, Robins A, Toy N (2002) A wind tunnel investigation of the influence of solar-induced wall-heating on the flow regime within a simulated urban street canyon. *Water Air Soil Pollut Focus* 2:555–571
21. Li X-X, Leung DY, Liu C-H, Lam K (2008) Physical modeling of flow field inside urban street canyons. *J Appl Meteorol Climatol* 47:2058–2067
22. Li X-X, Liu C-H, Leung DY, Lam K (2006) Recent progress in CFD modelling of wind field and pollutant transport in street canyons. *Atmos Environ* 40:5640–5658
23. Lim HC, Castro IP, Hoxey RP (2007) Bluff bodies in deep turbulent boundary layers: Reynolds-number issues. *J Fluid Mech* 571:97–118
24. Louka P, Belcher S, Harrison R (2000) Coupling between air flow in streets and the well-developed boundary layer aloft. *Atmos Environ* 34:2613–2621
25. Louka P, Vachon G, Sini J-F, Mestayer P, Rosant J-M (2002) Thermal effects on the airflow in a street canyon—Nantes’ 99 experimental results and model simulations. *Water Air Soil Pollut Focus* 2:351–364
26. Magnusson S, Dallman A, Entekhabi D, Britter R, Fernando HJ, Norford L (2014) On thermally forced flows in urban street canyons. *Environ Fluid Mech* 14:1427–1441. <https://doi.org/10.1007/s10652-014-9353-4>
27. Memon RA, Leung D (2011) On the heating environment in street canyon. *Environ Fluid Mech* 11:465–480
28. Meroney RN, Pavageau M, Rafailidis S, Schatzmann M (1996) Study of line source characteristics for 2-D physical modelling of pollutant dispersion in street canyons. *J Wind Eng Ind Aerodyn* 62:37–56
29. Nakamura Y, Oke TR (1988) Wind, temperature and stability conditions in an east-west oriented urban canyon. *Atmos Environ* 1967 22:2691–2700
30. Offerle B, Eliasson I, Grimmond C, Holmer B (2007) Surface heating in relation to air temperature, wind and turbulence in an urban street canyon. *Bound Layer Meteorol* 122:273–292
31. Oke T (1987) *Boundary layer climates*, 2nd edn. Methuen, London and New York
32. Santamouris M, Papanikolaou N, Koronakis I, Livada I, Asimakopoulos D (1999) Thermal and air flow characteristics in a deep pedestrian canyon under hot weather conditions. *Atmos Environ* 33:4503–4521
33. Snyder WH (1981) *Guideline for fluid modeling of atmospheric diffusion*. Environmental Protection Agency, Research Triangle Park
34. Uehara K, Wakamatsu S, Ooka R (2003) Studies on critical Reynolds number indices for wind-tunnel experiments on flow within urban areas. *Bound Layer Meteorol* 107:353–370
35. Vardoulakis S, Fisher BE, Pericleous K, Gonzalez-Flesca N (2003) Modelling air quality in street canyons: a review. *Atmos Environ* 37:155–182
36. Xie X, Huang Z, Wang J (2005) Impact of building configuration on air quality in street canyon. *Atmos Environ* 39:4519–4530
37. Yamartino RJ, Wiegand G (1986) Development and evaluation of simple models for the flow, turbulence and pollutant concentration fields within an urban street canyon. *Atmos Environ* 1967 20:2137–2156
38. Zajic D, Fernando H, Calhoun R, Princevac M, Brown M, Pardyjak E (2011) Flow and turbulence in an urban canyon. *J Appl Meteorol Climatol* 50:203–223
39. Zajic D, Fernando HJ, Brown MJ, Pardyjak ER (2015) On flows in simulated urban canopies. *Environ Fluid Mech* 15:275–303. <https://doi.org/10.1007/s10652-013-9311-6>